PROCEEDINGS OF SCIENCE

Weak Nuclear Statistical Equilibrium and the Production of Neutron-Rich Iron-Group Isotopes

Tianhong Yu[*]
Clemson Univerisity
E-mail: tyu@clemson.edu

Bradley S. Meyer[†‡]
Clemson University
E-mail: mbradle@clemson.edu

Calcium-48, ^{50}Ti, and ^{54}Cr are neutron-rich iron-group isotopes that show roughly correlated excesses and deficits in certain calcium-aluminum-rich inclusions (CAIs) in primitive meteorites. These isotopes are produced in high-temperature, low-entropy-per-nucleon environments such that the nuclear population are governed by a quasi-statistical equilibrium with too many heavy nuclei compared to nuclear statistical equilibrium. Such environments are present in dense thermonuclear (Type Ia) supernovae. Production of these isotopes also requires an electron fraction Y_e approximately equal to 0.42, which is set by electron captures during the explosion. We use NucNet Tools, an open-source suite of tools for nucleosynthesis, to study nucleosynthesis in high-density, low-entropy environments appropriate for Type Ia supernovae and follow the neutronization of the matter by weak interactions. We study how the nuclear populations evolve towards and into dynamical weak statistical equilibrium. Realistic expansion timescales for dense Type Ia supernova matter do not allow the material to reach dynamical weak statistical equilibrium. Nevertheless, such expansions are able to generate low enough Y_e to produce ^{48}Ca. The conditions in these expansions are extreme and thus probably rare in Galactic history, but, when they do occur, they produce copious amounts of ^{48}Ca and the other neutron-rich species. For this reason, it is likely that the abundance of these isotopes in interstellar dust is quite heterogeneous. Because the CAIs formed from interstellar dust precursors, they inherited this heterogeneity.

XII International Symposium on Nuclei in the Cosmos,
August 5-12, 2012
Cairns, Australia

[*]Supported by a NASA Earth and Space Science Fellowship.
[†]Speaker.
[‡]Supported by NASA Grant NNX10AH78G.

PoS(NIC XII)213

1. Introduction

Primitive Solar System hibonites and FUN (Fractionated and Unknown Nuclear effects) CAIs (calcium-aluminum-rich inclusions) show correlated excesses and deficits in neutron-rich iron-group elements (e.g., [1]). These isotopes are robustly produced in low-entropy expansions of neutron-rich matter [2], and such expansions likely occur in rare, dense, thermonuclear (Type Ia) supernovae [3].

In this brief paper we explore several low-entropy expansions and follow the neutronization that occurs due to weak interactions on free nucleons and nuclei. We compare network calculations to corresponding calculations of dynamical weak statistical equilibrium to study the extent to which the network calculations attain this equilibrium. For realistic supernova timescales, the expansions do not attain dynamical weak statistical equilibrium, but they do reach a degree of neutron richness sufficient to make neutron-rich iron-group isotopes like ^{48}Ca, ^{50}Ti, and ^{54}Cr.

2. Dynamical Weak Nuclear Statistical Equilibrium

Given sufficient time, a system undergoing nucleosynthesis can evolve until the nuclear species are in full equilibrium under assembly from free nucleons. This is the condition of nuclear statistical equilibrium (NSE), for which the chemical potential for a nuclear species with atomic number Z and mass number A is related to that for free neutrons (μ_n) and free protons (μ_p) by

$$\mu(Z,A) = Z\mu_p + (A-Z)\,\mu_n. \tag{2.1}$$

A related equilibrium is quasi-statistical equilibrium (QSE) in which nuclei are in equilibrium under exchange of nucleons, but the total number of heavy nuclei ($Z > 2$) is not that required by NSE because the three-body reactions assembling heavy nuclei are too slow [2]. In this case, the chemical potential for a heavy nucleus is given by

$$\mu(Z,A) = \mu_h + Z\mu_p + (A-Z)\,\mu_n. \tag{2.2}$$

where μ_h is the chemical potential of the heavy nuclei as a whole.

The NSE and QSE described above consider the total neutron-to-proton ratio to be fixed. Weak interactions can change this quantity so that the system can evolve to weak equilibrium. If neutrinos are trapped in the material, the system can evolve to weak nuclear statistical equilibrium (here called WSE) such that there is an equilibrium under the interchange of neutrons and protons via weak reactions. In this case there is the additional condition relating the chemical potentials of protons, electrons, neutrons, and electron-type neutrinos:

$$\mu_p + \mu_e = \mu_n + \mu_{\nu_e} \tag{2.3}$$

In WSE, nuclear abundances per nucleon $Y(Z,A)$ evolve until their chemical potentials satisfy Eq. (2.1) and the electron-to-nucleon ratio $Y_{\rm e}$ satisfies Eq. (2.3).

Densities are typically not sufficient in white dwarf star cores to trap neutrinos, however. In such matter, nuclear populations evolve not to WSE but rather to a dynamical weak nuclear statistical equilibrium (here called dWSE) [4]. In this case, the nuclear abundances obey Eq. (2.1), but

the constraint on the electron-to-nucleon ratio Y_e is instead given by the condition that the time rate of change of $Y_e = 0$. Because of the extremely low abundance of positrons in degenerate material, positron capture and β^+ decay are both small in white-dwarf star matter so that this dWSE arises when the total electron capture rate in the matter (which decreases Y_e) equals the total β^- decay rate (which increases Y_e).

3. Network Calculation

We study the nucleosynthesis of matter expanding from high temperature and density using NucNet Tools, an open-source suite of tools we have written to study nucleosynthesis [5]. Our network calculations use reaction rates from the Joint Institute for Nuclear Astrophysics database at http://www.jinaweb.org. We supplement these rates with weak-interaction rates from [6]. For nuclei that do not yet have microscopic weak rate estimates available, we use the approximate rate formulation in [4].

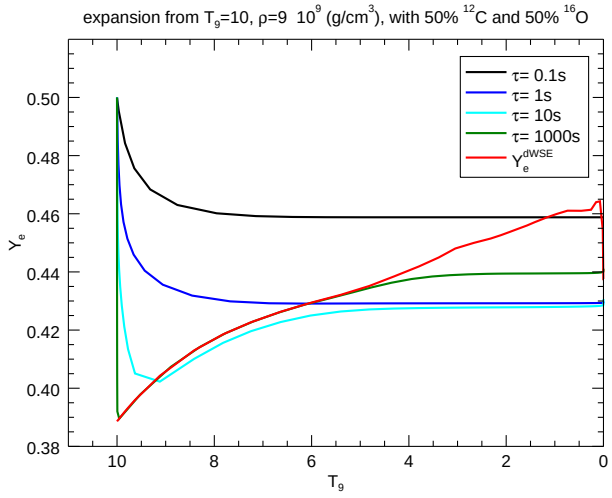

Figure 1: The evolution of the electron-to-nucleon ratio Y_e as a function of $T_9 = T/10^9$ K in expansions of various density e-folding timescale τ. Also shown as the red curve is the dynamical weak statistical equilibrium (dWSE) Y_e for the corresponding density and temperature. The slow expansions come close to attaining dWSE at high temperature and density but diverge from dWSE at lower temperature when the weak rates decrease dramatically. The faster expansions never attain dWSE.

We ran a set of calculations that began with 50% by mass of ^{12}C and 50% by mass ^{16}O. The matter began at a mass density ρ of 9×10^9 g cm^{-3} and a temperature of $T_9 = T/10^9\mathrm{K} = 10$. We considered the density to expand exponentially with time t such that $\rho(t) = \rho(0)\exp(-t/\tau)$, where τ is the density e-folding timescale. We considered the entropy of the matter to be dominated by relativistic particles such that $\rho \propto T_9^3$. We also ran some more detailed models that account for energy generation that we will describe in a future paper. These models show that $\rho \propto T_9^3$ is a reasonable parameterization for these studies.

Fig. 1 shows the time evolution of the electron-to-nucleon ratio Y_e for $\tau = 0.1, 1, 10$, and 1000 seconds. Also shown on this curve is the instantaneous dWSE value of Y_e. This is the electron-to-nucleon ratio the matter would evolve to if the expansion were arrested and the matter allowed to evolve at the fixed temperature and density at that point in the expansion. This quantity is computed by finding the value of Y_e at that temperature and density such that the NSE has a rate of change of Y_e equal to zero. The dWSE Y_e is low ($Y_e \approx 0.38$) early in the calculation because the density and, hence, the electron chemical potential is high. This favors electron capture and drives the dWSE Y_e down. As the matter expands and cools, the density drops. This lowers the electron chemical potential, which lowers the typical electron-capture rate and increases the dWSE Y_e.

As Fig. 1 shows, slow expansion (large τ) allows the system Y_e to keep pace with the dWSE Y_e better than the faster expansions. For $\tau = 1000$ s, the matter attains dWSE at $T_9 = 10$ and evolves in dWSE until the network diverges from dWSE near $T_9 = 5$ and freezes out at about $T_9 = 4$. In contrast, the faster expansions experience a drop from the initial $Y_e = 0.5$ early due to electron capture but freezeout near their final Y_e at about $T_9 = 8$.

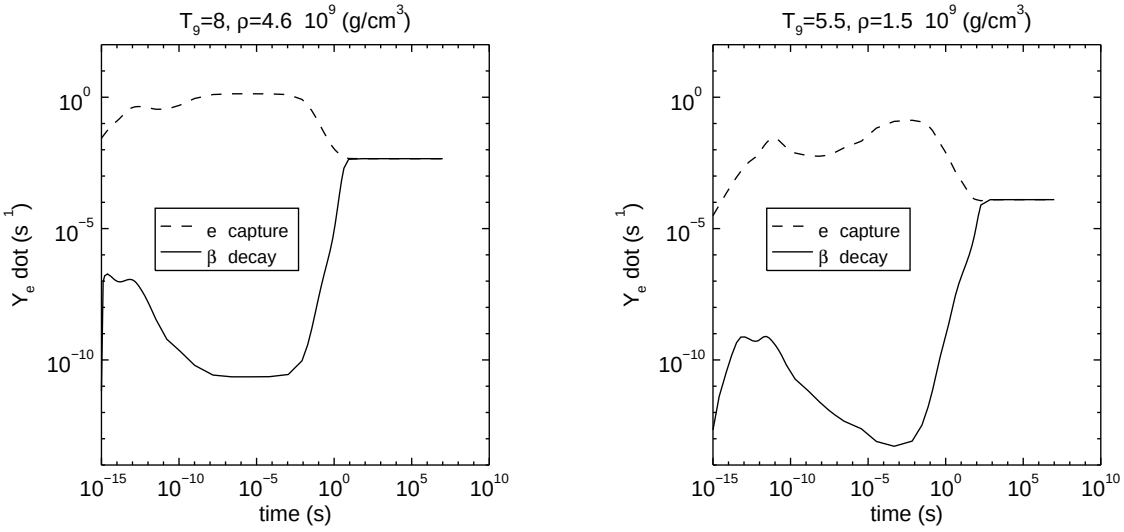

Figure 2: The total electron-capture and β^- decay rates as a function of time during the fixed temperature and density calculations. The system attains dWSE when the two rates become equal. Note that the lower density calculation takes a longer time to reach dWSE because the overall rates are lower.

To study the evolution of Y_e during these calculations, we made two calculations of matter with initial mass fractions of 50% ^{12}C and 50% ^{16}O evolving at fixed temperature and density drawn from points in the expansions shown in Fig. 1. The first calculation is for $T_9 = 8$ and $\rho = 4.6 \times 10^9$ g cm^{-3}. The left panel of Fig. 2 shows the total electron capture and total β^- decay rate during this calculation. Initially electron capture dominates beta decay and causes the Y_e to drop. As the material becomes neutron rich, however, β^- decay becomes important. After ~ 10 s, the total electron capture rate equals the total β^- decay rate and the matter attains dWSE. This explains why both the $\tau = 10$ s and $\tau = 1000$ s expansions are near dWSE at $T_9 = 8$ – the expansion timescale is longer than or comparable to the timescale to attain dWSE.

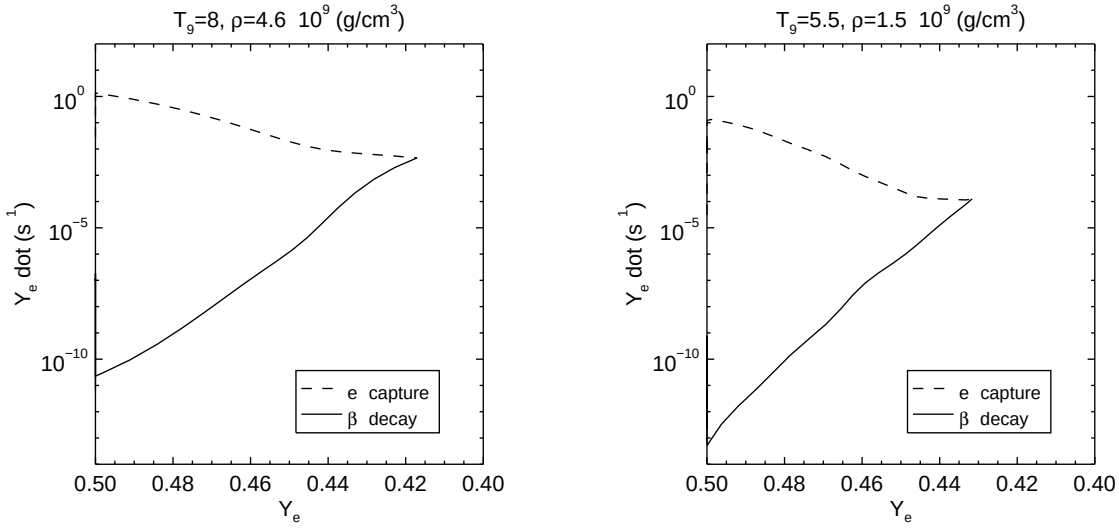

Figure 3: The total electron-capture and β^- decay rates as a function of the material's electron-to-nucleon ratio Y_e during the fixed temperature and density calculations. Initially the electron captures dominate β^- decay. As the material becomes more neutron rich, the β^- decay rates increase and the electron-capture rates decrease. When they become equal, the rate of change of Y_e becomes zero and the material reaches dWSE.

The second calculation is for $T_9 = 5.5$ and $\rho = 1.5 \times 10^9$ g cm^{-3}. The right panel of Fig. 2 shows the total electron capture and β^- decay rates for this calculation. This figure is similar to that for the previous calculation. The difference is that the overall rates are smaller because of the lower density (and electron chemical potential) which results in a longer timescale for evolution to dWSE (larger than ~ 100 s). The long timescale for evolution to dWSE means that, even for the $\tau = 1000$ s expansion, the network has difficulty keeping pace with the changing dWSE Y_e at this temperature and density.

Fig. 3 shows the total electron capture and β^- decay rates for the two fixed temperature and density calculations as a function of Y_e instead of time. This figure shows how, as the material neutronizes, the total electron capture rate declines and the total β^- decay rate increases. Once they meet, the rate of change of Y_e goes to zero and the system reaches dWSE.

Four movies that accompany this paper show the evolution of the elemental abundances in the four expansions as compared to those in QSE, NSE, and dWSE. Two other movies show the evolution of the elemental abundances for the two fixed temperature and density calculations. In the movies, it is clear that the nuclear populations evolve quickly into QSE, then NSE, and finally, on a longer timescale (if the expansion is not too fast), into dWSE.

Fig. 4 shows the mass fractions of the most abundant species in the $\tau = 1$ s expansion. This timescale is comparable to the explosion timescales expected in Type Ia supernovae. The dominant products are clearly ^{66}Ni, ^{60}Fe, ^{50}Ti, ^{48}Ca, and ^{54}Cr. These five species constitute nearly 86% of the mass from this expanding matter. About 14% of the final mass is in ^{48}Ca. Expansions from lower density do not reach as low a Y_e and, hence, produce much less ^{48}Ca. This result confirms that ^{48}Ca production is robust when high densities and timescales of seconds are present in expanding

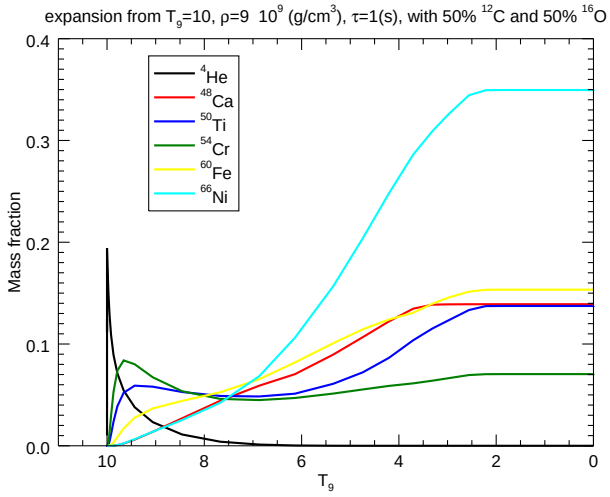

Figure 4: Mass fractions as a function of T_9 in the $\tau = 1$ s expansion.

matter.

4. Conclusion

Significant production of ^{48}Ca in expansions of low-entropy matter requires $Y_e \approx 0.42$. As we showed, densities near $\rho = 9 \times 10^9$ g cm^{-3} and expansion timescales of ~ 1 s can drive matter with $Y_e \approx 0.5$ down to this level and lead to robust ^{48}Ca synthesis. This occurs despite the fact that such relatively fast expansions never attain dynamical weak statistical equilibrium.

While Type Ia supernovae are fairly frequent events in the Galaxy and significant producers of the Solar System's supply of iron, a density as high as 9×10^9 g cm^{-3} is rare in white dwarf stars (e.g., [3]), the progenitors of these explosions. This means that Type Ia supernova production of ^{48}Ca is probably rare. Nevertheless, as our calculation shows, these rare events would make tremendous amounts of ^{48}Ca. Because of this, our expectation is that this isotope is rather heterogeneously distributed in the dust in the interstellar medium. When such dust was inherited by the early Solar nebula, the isotopically heterogeneous dust formed into solids such as hibonites and FUN CAIs, which then naturally show isotopic anomalies in the neutron-rich iron-group isotopes.

References

[1] Meyer, B. S., & Zinner, E. 2006, Meteorites and the Early Solar System II, 69

[2] Meyer, B. S., Krishnan, T. D., & Clayton, D. D. 1996, *Ap. J.* 462, 825

[3] Woosley, S. E. 1997, *Ap. J.* 476, 801

[4] Arcones, A., Martínez-Pinedo, G., Roberts, L. F., & Woosley, S. E. 2010, *Astron. Ap.* 522, A25

[5] Available at http://sourceforge.net/projects/nucnet-tools.

[6] Langanke, K., & Martínez-Pinedo, G. 2001, *Atomic Data and Nuclear Data Tables* 79, 1